Shock loading of layered materials with SPH

Shock loading of layered materials with SPH

Iason Zisis[1,2]
Materials Innovation Institute, M2i[1]
Delft, The Netherlands
i.zisis@tue.nl

Bas van der Linden[2]
Dept. of Mathematics and Computer Science[2]
Eindhoven University of Technology
Eindhoven, The Netherlands

***Abstract* — Hypervelocity impacts into structures produce shock waves propagating through the colliding bodies. SPH has given insight into shock loading of homogeneous materials; nevertheless, shock wave propagation through solids with discontinuous density distribution, has not been considered in depth, yet. In previous studies using SPH, impact loading of laminated or composite materials was modeled by homogenization of the structure or under the assumption of being functionally graded materials. Both models neglect the reflection-transmission effects on the interface of different density materials. To capture these reflection-transmission effects, a holistic treatment for the multi-phase material is proposed, with kernel interaction over all parts of the structure. The algorithm employs a variable smoothing length formulation. A dissipative mass flux term is also introduced in order to remove spurious post-shock oscillations on the interface of different materials. In this paper, the SPH solution is presented, along with a relevant benchmark case. The algorithm's performance is studied and the necessity of a variable smoothing length formulation is investigated.**

I. INTRODUTION

The shields of spacecraft in orbit experience impacts by small sized particles of space debris which travel at speeds of 10km/s. These Hypervelocity Impacts (HVIs) are characterized by the projectile's velocity being higher than the target's material speed of sound. Sharp density changes occur, propagated through the target as shock waves. Normal stress effects on an incremental element of the material overweight the deviatory stress effects and hydrodynamic loading regime occurs [1, 2]. Solid materials will effectively behave like fluids in this loading regime. HVIs are typical processes involving extreme compressibility effects of solids, making them substantially different than ballistic impacts.

The efficiency of Smoothed Particle Hydrodynamics (SPH) in simulating HVIs was exhibited in the original simulation of HVI events into monolithic materials by Libersky et al. [3]. Later combined numerical and experimental works established the method as the state-of-the-art tool for HVI simulations [4,5]. Within SPH's context, disintegration of materials under impact is described without severe algorithmic complexity, compared to other methods like Finite Elements Method (FEM) [2].

Shields of multi-material structures have a lower weight-to-performance ratio and are preferred to monolithic ones [6]. SPH was also used to simulate HVIs into multi-component structures [7-9]. Johnson et al. [10] suggested a special interface algorithm to treat non-bonded interfaces (e.g. projectile/target), claiming that when two bodies exchange momentum through simple SPH kernel interaction large errors are produced; this observation was also studied by Campbell et al. [11]. Homogenized materials were introduced in [7-9], with properties the averaged properties of their components. A rigorous procedure of producing averaged versions of anisotropic materials [2,7-9]. Nevertheless, two major drawbacks are apparent in this approach: the homogenization process is based on assumptions coming from quasi-static loading regimes, and the effects of shock reflection-transmission are neglected.

In the case of layered composite materials, shock waves will not propagate undisturbed through the specimen. The transition from one layer to its adjacent layer is not a smooth function of space; it shows up as a discontinuity in the density distribution of the target and reflections-transmissions will occur, whenever a shock encounters a material interface [12]. Hence, the shock loading problem becomes a multiphase shock problem.

SPH algorithms for multi-phase simulations focus on incompressible flow regimes [13-15]. In another approach, the Modified-SPH method is introduced [16] to solve an elastic wave propagation problem through a functionally graded material. The properties of such a material are smooth functions of space. Therefore, without any discontinuities in the properties of the material it is impossible for any transmission-reflection pattern to occur.

The type of artificial viscosity introduced by Monaghan and Ginold [17] is used in all previously mentioned studies. It is a popular way to remove the spurious oscillations in the vicinity of the shocks. An alternative shock capturing technique is the implementation of a Riemann solver in the SPH scheme; such SPH algorithms are described by Intuska [18] and Cha et al. [19]. In a similar manner, an SPH scheme based on the acoustic approximation of the Riemann problem is developed by Parshikov et al. [20].

In this paper, an SPH formulation is discussed that is able to simulate shock loading of a material with purely discontinuous properties. It is based on artificial dissipation techniques. A new artificial term is added to the discretized continuity equation, which smoothens out unphysical blips occurring from shocks on interfaces of materials. It is tested upon a one dimensional benchmark case. The modified scheme conserves momentum exactly and captures the transmission-reflection of shocks on interfaces of materials.

II. Mathematical Model

A. Governing equations

The governing equations for HVIs are the conservation of mass, momentum and energy, which in a Lagrangian frame of reference write:

$$\frac{D\rho}{Dt} = -\rho\frac{\partial u^\alpha}{\partial x^\alpha}\,,\ \frac{Du}{Dt} = \frac{1}{\rho}\frac{\partial \sigma^{\alpha\beta}}{\partial x^\alpha}\,,\ \frac{De}{Dt} = -\frac{\sigma^{\alpha\beta}}{\rho}\frac{\partial u^\alpha}{\partial x^\beta}\,,$$
$$\frac{dx^\alpha}{dt} = u^\alpha \quad \text{for } \alpha,\beta = 1,2,3\,. \tag{1}$$

In (1) superscripts indicate the directional index and stresses σ are composed by a normal and a deviatoric part as $\sigma^{\alpha\beta} = -p\delta_{\alpha\beta} + \tau^{\alpha\beta}$, where $\delta_{\alpha\beta}$ is the Kronecker delta.

A simplified model of (1) to benchmark algorithms related to shock effects are the Euler equations. They describe the flow of compressible media, allowing for shock formation. Opting for a simple paradigm, system (1) is reduced to one spatial dimension and thermal processes are neglected, giving:

$$\frac{D\rho}{Dt} = -\rho\frac{\partial u}{\partial x}\,, \qquad \frac{Du}{Dt} = -\frac{1}{\rho}\frac{\partial p}{\partial x}\,, \qquad \frac{dx}{dt} = u\,. \tag{2}$$

Since in one dimension only "normal" stresses p are exerted, no distinction can be made between fluids and solids. The following linear Equation of State (EoS), describes a compressible elastic structure, consisting of a spatially varying bulk modulus constant in time. Pressure from a reference density $\rho_o = \rho(x,0)$ is measured [2] as:

$$p(x,t) = K(x)\left(\frac{\rho(x,t)}{\rho(x,0)} - 1\right), \tag{3}$$

B. Non-dimensionalization

The following dimensionless magnitudes transform (2) into its non-dimensional form:

$$x^* := x/L\,,\ t^* := t/\tau\,,\ u^* := u/u_o,$$
$$\rho^* := \rho/\rho_o\,,\ p^* := p/p_o\,. \tag{4}$$

Choosing timescale $\tau = L/u_o$ and pressure scale $p_o = \rho_o u_o^2 = \rho(x,0)u_o^2$ the non-dimensional form of (2) is identical to itself. Dividing (3) by p_o, the non-dimensional EoS becomes:

$$p^* = \frac{K(x)}{\rho(x,0)u_o^2}(\rho^* - 1) = \frac{1}{\mathrm{Ca}(x)}(\rho^* - 1)\,, \tag{5}$$

where

$$\mathrm{Ca}(x) := \frac{\rho(x,0)u_o^2}{K(x)} \tag{6}$$

is the Cauchy number. It is a spatially varying dimensionless quantity, measuring the ratio of the initial inertial forces over the resistance of the materials to compression.

After removing all asterisks, the system of equations looks similar to (2):

$$\frac{D\rho}{Dt} = -\rho\frac{\partial u}{\partial x}\,, \qquad \frac{Du}{Dt} = -\frac{1}{\rho}\frac{\partial p}{\partial x}\,, \qquad \frac{dx}{dt} = u\,, \tag{7a}$$

$$p(x,t) = \frac{1}{\mathrm{Ca}(x)}(\,\rho(x,t) - 1\,)\,. \tag{7b}$$

Given the compressibility effects produced by the projectile's inertia on the target, the bulk modulus $K(x)$ scales with the dynamic pressure at the moment of impact. Therefore, a suitable choice for the velocity scale is $u_o = u_{\mathrm{impact}}$; the relative velocity at which projectile and target travel.

Typical length scales of targets in HVIs are in the order of millimeters to centimeters [6]. Velocity scales with the relative impact velocity u_{impact}. Considering a HVI of u_{impact} = 10 km/s and L = 1 cm, the time-scale is brought down to τ = 1 μsec. As an example, for Aluminum 2045-T4 the magnitude of Ca for a 10 km/s impact is computed; with a nominal density ρ_o = 2,700 kg/m^3 and K = 73 GPa, Ca = 3.7 is found, according to (6).

The material's non-dimensional speed of sound c is defined in [2] as:

$$c(x) = \sqrt{dp/d\rho} = \mathrm{Ca}(x)^{-1/2}\,. \tag{8}$$

III. SPH Discretization

A. Discretization of equations

The continuity equation formulation of SPH writes:

$$\left(\frac{D\rho}{Dt}\right)_i = \rho_i \sum_{j=1}^{N} \frac{m_j}{\rho_j}(u_i - u_j)\frac{\partial W_{ij}}{\partial x_i}\,. \tag{9}$$

Not all combinations of continuity and momentum SPH discretizations furnish momentum conserving schemes. The coupling of the continuity equation with the following momentum discretization was shown to conserve mass and momentum exactly [15,21]:

$$\left(\frac{Du}{Dt}\right)_i = -\frac{1}{\rho_i}\sum_{j=1}^{N} \frac{m_j}{\rho_j}(p_i + p_j)\frac{\partial W_{ij}}{\partial x_i}\,. \tag{10}$$

B. Varying smoothing length formulation

The above discretization of balance equations has been used to simulate multiphase phenomena in the incompressible regime [15]. However, when severe compression effects are studied, particle spacing varies substantially. Since particle spacing affects the SPH interpolation, the resolution of the scheme is corrupted. A solution to this is to rescale the interpolation kernel according to a spatially varying smoothing length. It should automatically increase as the particle system expands and decrease as it contracts [22].

Several smoothing length variations have been proposed, without all of them furnishing a scheme variationally consistent [22]. In the formulations by Price [23] and Monaghan [22], the smoothing length varies with density as:

$$h_i = \eta \frac{m_i}{\rho_i} \ , \tag{11}$$

where η =1.2 (following [23]) and the interpolation kernel is scaled with the factor:

$$\Omega_i = 1 - \frac{\partial h_i}{\partial \rho_i} \sum_{j=1}^{N} m_j \frac{\partial W_{ij}(h_i)}{\partial h_i} \ . \tag{12}$$

For the system of (9) and (10), the following modification is proposed.

$$\left(\frac{D\rho}{Dt}\right)_i = \frac{\rho_i}{\Omega_i} \sum_{j=1}^{N} \frac{m_j}{\rho_j} (u_i - u_j) \frac{\partial W_{ij}(h_i)}{\partial x_i} \ , \tag{13}$$

$$\left(\frac{Du}{Dt}\right)_i = -\frac{1}{\rho_i} \sum_{j=1}^{N} \frac{m_j}{\rho_j} \left(\frac{p_i}{\Omega_i} \frac{\partial W_{ij}(h_i)}{\partial x_i} + \frac{p_j}{\Omega_j} \frac{\partial W_{ij}(h_j)}{\partial x_i} \right) . \tag{14}$$

The system is closed with a particle based calculation of the pressure and the position change.

$$p_i = \frac{1}{\mathrm{Ca}_i} (\rho_i - 1) \ , \tag{15}$$

$$\frac{dx_i}{dt} = u_i \ . \tag{16}$$

C. Interpolation kernel

The Gaussian function is chosen as the interpolation kernel, with a scaling such that $\sum_1^N W(\mathbf{x}_i - \mathbf{x}_j, h)\, V_j = 1$ inside the computational domain:

$$W_{ij} = \frac{1}{h\sqrt{\pi}} exp\left\{ -\left(\frac{x_i - x_j}{h}\right)^2 \right\} \ , \tag{17}$$

where h is the smoothing length.

D. Initialization and time integration

For the cases tackled in this paper, free boundary conditions are considered, discontinuous initial data and a discontinuous parameter Ca.

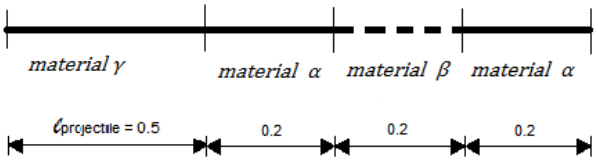

Figure 1. Initial configuration of the materials

TABLE I. Material's initial positions and velocities

Material	Initial position x_o	Velocity u
α	$0.5 \le x_o < 0.7$	0
β	$0.9 \le x_o < 1.1$	0
γ	$0 \le x_o < 0.5$	1

The initial configuration of the materials is depicted in Fig.1, where the length of the projectile $\ell_{\text{projectile}}$ is chosen large enough so that no effects from rebounded waves occur. Combined with the initial data of Table 1, a velocity-induced shock is described.

The SPH particle system is initialized by distributing N particles over the domain that the materials initially occupy (Table 1). The initial interparticle distances are taken to be of equal length δx_o. Particles of materials with different density, α and β, have proportional masses as $m_\alpha/m_\beta = \rho_\alpha/\rho_\beta$; these, remain constant in time.

After a number of particles per unit length n_ℓ is defined, the particles are distributed over initial positions $x_{o,i}$, according to the following scheme:

$$\delta x_o = \ell / n_\ell \ , \qquad x_{o,i} = \delta x_o (i-1) \ . \tag{18}$$

where ℓ is the total length of the computational domain considered.

Updates of variables and particle positions in time are achieved via the following scheme. Magnitudes are obtained in the order presented. Braces denote simultaneous update of the enclosed variables and superscripts are reserved for time steps, while subscripts for particle indices. The smoothing length is initially taken as $h_i^0 = \eta m_i / \rho_i^0$. Advancing half a time-step for density and velocity from the initial conditions:

$$\{\rho, u\}_i^{1/2} = \{\rho, u\}_i^0 + \frac{1}{2} \delta t \left(\frac{D\{\rho, u\}}{Dt} \right)_i^0 \tag{19a}$$

and a full-step for position:

$$x_i^1 = x_i^0 + \delta t \, u_i^{1/2} \ . \tag{19b}$$

At every subsequent time step k variables are updated according to:

$$\{\rho,u\}_i^k = \{\rho,u\}_i^{k-1/2} + \frac{1}{2}\delta t\left(\frac{D\{\rho,u\}}{Dt}\right)_i^{k-1}, \qquad (19c)$$

$$h_i^k = \eta\frac{m_i}{\rho_i^k}, \qquad (19d)$$

from which $\left(\frac{D\{\rho,u\}}{Dt}\right)_i^k$ is calculated for each i-th particle according to (11) − (15).

$$\{\rho,u\}_i^{k+1/2} = \{\rho,u\}_i^{k-1/2} + \delta t\left(\frac{D\{\rho,u\}}{Dt}\right)_i^k, \qquad (19e)$$

$$x_i^{k+1} = x_i^k + \delta t\, u_i^{k+1/2}. \qquad (19f)$$

A limit to the time-step size is set by the CFL criterion, which by taking the smoothing length as the shortest spatial scale (similarly to [3,17]) gives:

$$\delta t \le \omega \min\left(\frac{h}{c_i + u^*_{\text{impact}}}\right), \qquad (20)$$

where $\omega \in (0, 1]$ is a "safety" parameter. The largest time-step allowed is found by computing c_i from (8) and the non-dimensional u^*_{impact}= 1 (u_{impact} is the velocity scale). For all calculations a constant $\delta t = 10^{-4}$ was sufficient.

IV. SHOCK CAPTURING

A. Artificial viscosity

In order to capture shocks in gas dynamic simulations with SPH, Price [23] and Monaghan [24] suggest a generalized way to construct dissipative terms for the balance equations (1). By Θ each variable on the left hand side of (1) is represented:

$$\left(\frac{D\Theta}{Dt}\right)_{i,diss} = \sum_{j=1}^{N} m_j \frac{\alpha_\Theta\, v^\Theta_{sig}}{\bar\rho_{ij}}\left(\Theta_i - \Theta_j\right) r_{ij}\,\overline{\left(\frac{\partial W_{ij}}{\partial x_\iota}\right)},$$

$$r_{ij} = \frac{x_i - x_j}{|x_i - x_j|}, \qquad \overline{\left(\frac{\partial W_{ij}}{\partial x_\iota}\right)} = \frac{1}{2}\left(\frac{\partial W_{ij}(h_i)}{\partial x_i} + \frac{\partial W_{ij}(h_j)}{\partial x_i}\right),$$

$$v^\Theta_{sig} = \frac{1}{2}\left(c_i + c_j - \beta\left(u_i - u_j\right) r_{ij}\right), \qquad (21)$$

where a_Θ and β are parameters and v^Θ_{sig} is the propagation speed of the information carried by the dissipative terms. These terms are frequently used to produce dissipation for the solution of the momentum and energy equations.

For the momentum equation in the case studied here the above expression is used for the velocity:

$$\left(\frac{Du}{Dt}\right)_{i,diss} = \sum_{j=1}^{N} m_j \frac{\alpha_u\, v^u_{sig}}{\bar\rho_{ij}}\left(u_i - u_j\right) r_{ij}\,\overline{\left(\frac{\partial W_{ij}}{\partial x_\iota}\right)},$$

$$v^u_{sig} = \frac{1}{2}\left(c_i + c_j - \beta\left(u_i - u_j\right)\right). \qquad (22)$$

B. Artificial dissipative mass flux

The following discussion, presents a new term, developed in order to smoothen out spurious blips in density and pressure, for a shock through a material interface.

Using equation (21), an artificial term is added in the discretized continuity equation (14):

$$\left(\frac{D\rho}{Dt}\right)_{i,diss} = \sum_{j=1}^{N} \frac{\alpha_\rho\left(p_i - p_j\right)}{\bar c_{ij}}\frac{m_j}{\rho_j} r_{ij}\,\overline{\left(\frac{\partial W_{ij}}{\partial x_\iota}\right)}. \qquad (23)$$

Unphysical oscillations occur in pressure, while density discontinuities are natural characteristics of inhomogeneous materials. Therefore, an expression in the same manner as (21) needs to account for pressure differences. Exploiting (14), (21) is written as:

$$m_j \frac{\alpha_\rho\, v^\rho_{sig}}{\bar\rho_{ij}}\left(\rho_i - \rho_j\right) = m_j \frac{\alpha_\rho\, v^\rho_{sig}}{\bar\rho_{ij}}\left(\frac{p_i}{c_i^2} - \frac{p_j}{c_j^2}\right), \qquad (24)$$

for $v^\rho_{sig} = v^u_{sig}$.

Averaging of the density of different materials is not favorable, because would smoothen material interfaces that are naturally present in the domain. Hence, $m_j/\bar\rho_{ij}$ is replaced with m_j/ρ_j and with a further approximation the final form is furnished:

$$m_j \frac{\alpha_\rho\, v^\rho_{sig}}{\bar\rho_{ij}}\left(\frac{p_i}{c_i^2} - \frac{p_j}{c_j^2}\right) \sim \frac{m_j}{\rho_j}\frac{\alpha_\rho\left(p_i - p_j\right)}{v^\rho_{sig}}, \qquad (23)$$

The dissipative term (23) introduces a mass flux into the system, smoothens out the spurious oscillations of density and pressure, occurring on the interface of two materials. Its effect is similar and complementary to the effect of (22).

V. RESULTS AND DISCUSSION

A simple test case is set up with the initial values appearing in Table 2. For all computations n_ℓ=400 particles per unit length were used.

TABLE II. Material's initial density and Ca number

Material	Density	Ca
α	1	1
β	0.5	0.25
γ	1	1

The discontinuous initial data of the test case constitute a Riemann problem. After the impact, two shocks appear; a left-travelling and a right travelling. The exact solution is given according to the procedures in Toro's book [25], considering the isothermal Euler equations and an equation of state of the form (7b).

In order to test the effectiveness of the artificial mass flux term, dissipation is first added only in the momentum equation according to (22). In Fig.2, the particle and continuous (particle values are cast in the SPH interpolation formula) values of density are plotted at t = 0.1. Particle spacing is well-preserved, due to the rescaling of the kernel; however, unphysical oscillations persist. This effect was underlined by Campbell et al. [11].

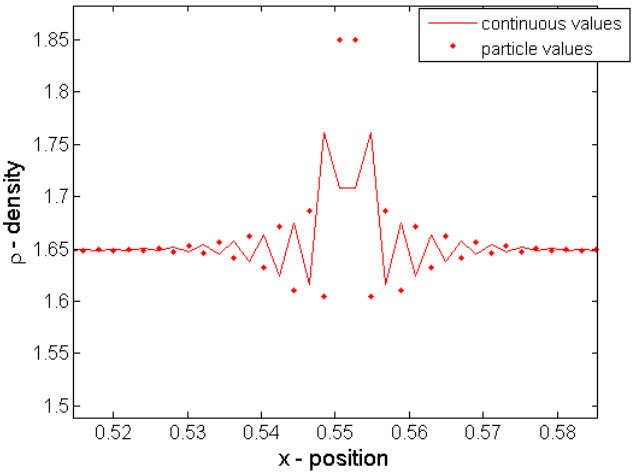

Figure 2. Density in the impact region at t = 0.1 .

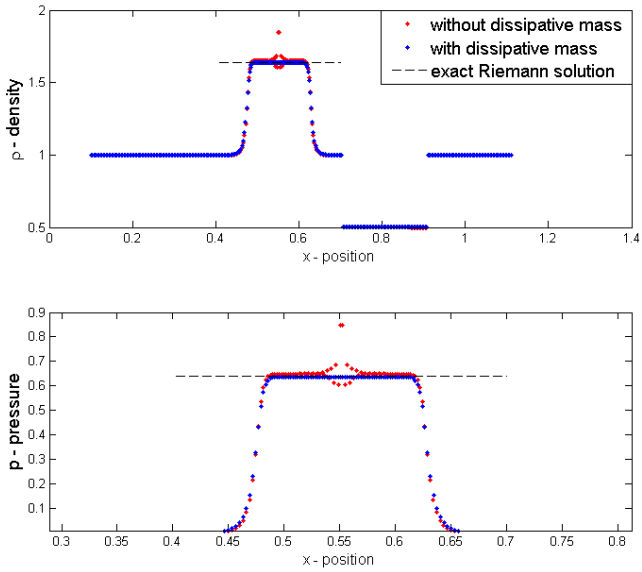

Figure 3. Density and pressure at t = 0.1 .

When the dissipative mass flux term (23) is added to the continuity equation with α_ρ = 0.4, the spurious oscillations of the solution at t = 0.1 disappear (Fig.3); both from density and pressure. Furthermore, the new term, does not affect the jumps in the material's density away from the shock, as is shown in the density distribution in Fig.3.

In Fig.3, the exact solution of the relevant Riemann problem (ρ_{exact}=1.640, p_{exact}=0.640) is also plotted with dotted line in Fig.3. The agreement with the SPH solution is remarkable. In particular, the dissipative mass flux term captures correctly the strength of the shock.

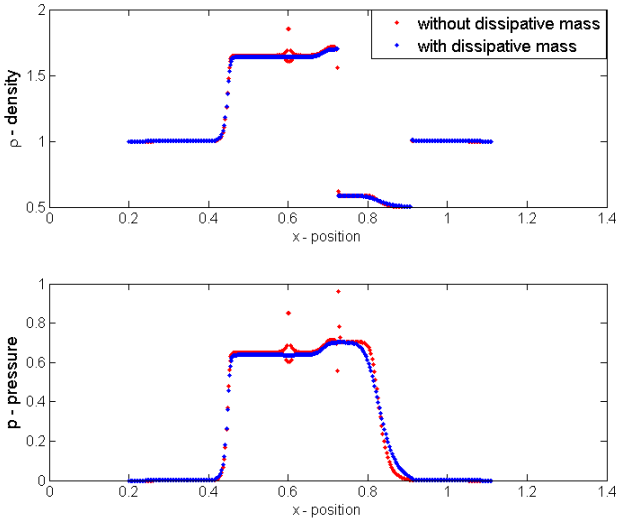

Figure 4. Density in the impact region at t = 0.2 .

At t = 0.2, the shock has already encountered the interface of the two materials (Fig.4). One wave is reflected back to material α and another is transmitted to material β. When dissipation is only added to the momentum equation, severe oscillations occur in the pressure distribution, in the vicinity of the two materials' interface. Additionally, the effects of the initial impact have not disappeared.

The effects of the dissipative mass term are clearly beneficial. Both materials experience the same pressure, as is expected on contact discontinuities emerging from the Riemann problem [25]. However, compared to the solution without dissipative mass flux, higher smoothening of the shock is observed.

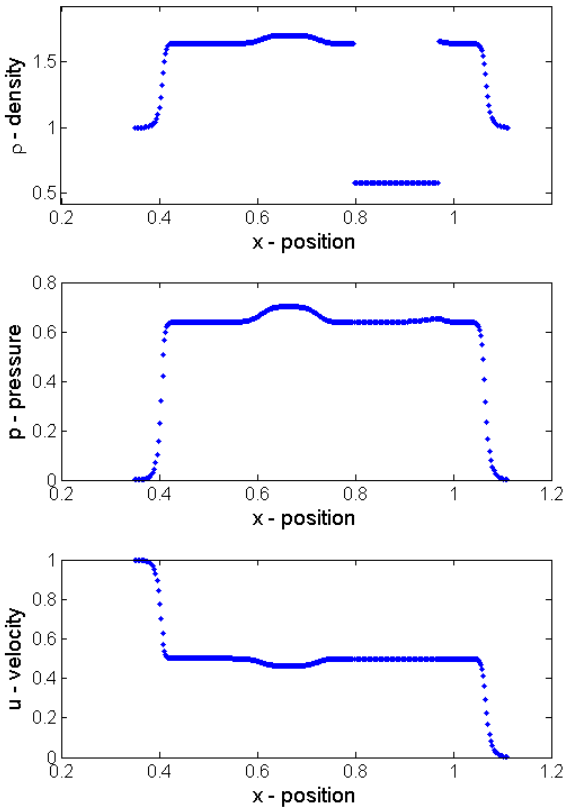

Figure 5. Density, pressure and velocity at $t = 0.35$.

At $t = 0.35$ (Fig.5) the initial left-running and right-running shocks arrive on the edges. Density has not changed on any edge, nor the velocity. Colliding waves have created a region of increased density and pressure to the right of $x = 0.6$. In the same region, velocity is decreased. The contact discontinuity on the interface β-α (near $x = 1$) was set to motion when the shock arrived. The value of pressure across it is not changing significantly, describing the physically relevant situation of a zero pressure gradient across it.

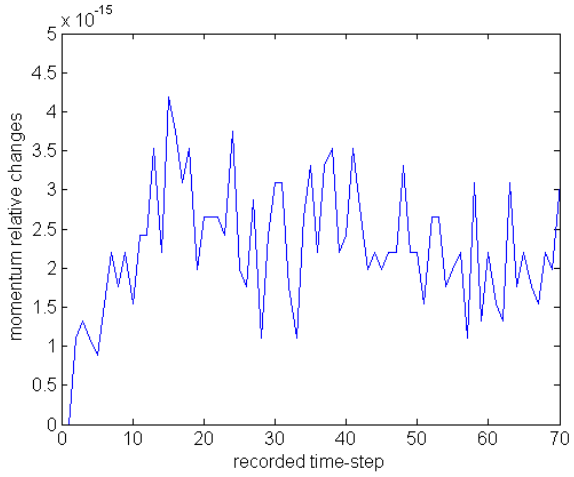

Figure 6. Relative changes in momentum from $t = 0$ to $t = 0.35$.

Finally, relative changes to momentum are calculated based on the particle velocity as:

$$\Delta M(t) = \left| \frac{J(t) - J(0)}{J(0)} \right| , \qquad J(t) = \sum_{i=1}^{N} m_i u_{i(t)} \quad (24)$$

and are plotted in Fig.6 for $t = 0$ to $t = 0.35$. Momentum changes are in the order of machine precision and therefore negligible. This fact, exhibits the momentum conservative property of the developed SPH scheme.

VI. Conclusions

In the present work a method was developed which removes spurious oscillations observed during shock loading of layered materials. It is an improvement to the ability of SPH to capture the reflection-transmission of shock waves on material interfaces. It is *holistic* approach, since every particle interacts only through its SPH kernel with the whole computational domain.

An artificial mass flux term was devised and combined with the varying smoothing length formulation of SPH. The scheme which was furnished was shown to be momentum conservative.

Further steps of development include the exploration of the proposed scheme's properties and limitations. Concerning the former, the complete solution of the Riemann problem will be enlightening. Additionally, the optimal value of the α_ρ parameter, is also a critical issue. The same holds for the limiting value of the materials' density ratio that can be incorporated by the scheme. Finally, since the term is based on a generic formulation, extension to more spatial dimensions is straightforward.

Acknowledgements

This research was carried out under project number M11.4.10412 in the framework of the Research Program of the Materials innovation institute M2i (www.m2i.nl). It is also a research activity of Sioux LIME bv. (www.limebv.nl).

References

[1] J.R. Asay and G.I. Kerley, "The response of materials to dynamic loading", International Journal of Impact Engineering,**5**, pp.69-99, 1984.

[2] S.J. Hiermaier, Structures Under Crash and Impact - Continuum Mechanics, Discretization and Experimental Characterization, Chap. 3, pp.75, Springer Science+Business Media, LLC, New York, 2008.

[3] L.D. Libersky, A.G. Petschek, T.C. Carney, J.R. Hipp, and F.A Allandadi, "High strainLagrangian Hydrodynamics: A three-dimensional SPH code for dynamic material response", Journal of computational Physics, **109**, pp.67-75,1993.

[4] S. Hiermaier, D. Konke, A.J. Stilp and K. Thoma, "Computational simulation of the hypervelocity impact of Al-spheres on thin plates

of different materials", International Journalof Impact Engineering, **20**, pp.363-374, 1997.

[5] C.J. Hayhurst, I.H. Livingstone, R.A. Clegg, G.E. Fairlie, S.J. Hiermaier and M. Lambert, "Numerical Simulation of Hypervelocity Impacts on Aluminum and Nextel/Kevlar Whipple Shields", Hypervelocity Shielding Workshop, 8-11 March 1998, Galveston, Texas.

[6] E.L. Christiansen, J.L. Crews, J.E. Williamsen, J.H. Robinson, and A.M. Nolen, "Enhanced meteoroid and orbital debris shielding", International Journal of Impact Engineering, **17**, pp.217-228, 1995.

[7] W. Riedel, H. Nahme, D. M. White & R.A. Clegg, "Hypervelocity Impact Damage Prediction in Composites Part I & II", International Journal of Impact Engineering, **33**(1–12), pp.670–680, 2006.

[8] R. Clegg, C. Hayhurst, J. Leahy, and M. Deutekom, "Application of a Coupled Anisotropic Material Model to High Velocity Impact Response of Composite Textile Armour", 18th International Symposium and Exhibition on Ballistics San Antonio, Texas USA, November 15-19 1999.

[9] M. Wicklein, S. Ryana, D.M. Whiteb, and R.A. Clegg, "Hypervelocity impact on CFRP: Testing, material modelling, and numerical simulation", International Journal of Impact Engineering,**35** (2008) pp.1861–1869.

[10] G.R. Johnson,R.A. Stryk and S.R. Beissel, "SPH for high velocity impact computations", Computer Methods in Applied Mechanics and Engineering, **139**, pp. 347-37, 1996.

[11] J. Campbell, R. Vignjevic, and L. Libersky, "A contact algorithm for smoothed particle hydrodynamics", Computer Methods in Applied Mechanicsand Engineering,**184**, pp. 49-65, 2000.

[12] L. Davison, , *Fundamentals of Shock Wave Propagation in Solids*, Chap. 8, pp.186-191, Springer-Verlag Berlin Heidelberg, 2008.

[13] X.Y. Hu, N.A. Adams, "A multi-phase SPH method for macroscopic andmesoscopic flows", Journal of Computational Physics,**213**, (2006) pp. 844–861.

[14] N. Grenier, M. Antuono, A. Colagrossi, D. LeTouzé and B. Alessandrini, "An Hamiltonian interface SPH formulation for multi-fluidand free surface flows", Journal of Computational Physics,**228,** pp.8380–8393, 2009.

[15] A. Colagrossi, and M. Landrini, "Numerical simulation of interfacial flows by smoothedparticle hydrodynamics", Journal of Computational Physics,**191**, pp.448–475, 2003.

[16] G.M. Zhang and R.C. Batra, "Wave propagation in functionally graded materials by modified smoothed particle hydrodynamics (MSPH) method", Journal of Computational Physics,**222**, pp.374–390, 2007.

[17] J.J. Monaghan, and R.A. Ginold, "Shock Simulation by the Particle Method SPH", journal of computational physics, **52**, pp. 374-389, 1983.

[18] S. Intuska, "Reformulation of Smoothed Particle Hydrodynamics with Riemann Solver", Journal of Computational Physics, **179**, pp.238-267, 2002.

[19] S.H. Cha and A.P. Whitworth, "Implementation and tests of Godunov-type particle hydrodynamics", Monthly Notices of the Royal Astronomical Society, **340**, pp. 73-90, 2003.

[20] A.N. Parshikov, and S.A. Medin, "Smoothed Particle Hydrodynamics UsingInterparticle Contact Algorithms", Journal of Computational Physics,**180**, pp.358–382 2002.

[21] J. Bonet and T.-S.L. Lok, "Variational and momentum preservation aspects of Smooth Particle Hydrodynamic formulations", Comput. Methods Appl. Mech. Engrg., 180, pp. 97-115, 1999.

[22] J.J. Monaghan, "Smoothed particle hydrodynamics", Rep. Prog. Phys., pp. 681-703, 2005.

[23] D.J. Price, "Modelling discontinuities and Kelvin-Helmholtz instabilities in SPH", Journal of Computational Physics, **227**, pp.10040-10057, 2008.

[24] J.J. Monaghan, "SPH and Riemann Solvers", Journal of Computational physics,**136**, pp.298–307, 1997.

[25] E.F. Toro, Riemann solvers and numerical methods for fluid dynamics: a practical introduction, 3rd edition, Springer-Verlag Berlin Haidelberg, 2009, pp.119-125.